Cell, Vol. 115, 37–48, October 3, 2003, Copyright ©2003 by Cell Press

Formation of an Endophilin-Ca^{2+} Channel Complex Is Critical for Clathrin-Mediated Synaptic Vesicle Endocytosis

Yuan Chen,[1] Lunbin Deng,[2] Yuka Maeno-Hikichi,[1] Meizan Lai,[1] Shaohua Chang,[1] Gong Chen,[2] and Ji-fang Zhang[1,*]
[1]Department of Pharmacology
University of Pennsylvania School of Medicine
3620 Hamilton Walk
Philadelphia, Pennsylvania 19104
[2]Department of Biology
Pennsylvania State University
University Park, Pennsylvania 16802

Summary

A tight balance between synaptic vesicle exocytosis and endocytosis is fundamental to maintaining synaptic structure and function. Calcium influx through voltage-gated Ca^{2+} channels is crucial in regulating synaptic vesicle exocytosis. However, much less is known about how Ca^{2+} regulates vesicle endocytosis or how the endocytic machinery becomes enriched at the nerve terminal. We report here a direct interaction between voltage-gated Ca^{2+} channels and endophilin, a key regulator of clathrin-mediated synaptic vesicle endocytosis. Formation of the endophlin-Ca^{2+} channel complex is Ca^{2+} dependent. The primary Ca^{2+} binding domain resides within endophilin and regulates both endophilin-Ca^{2+} channel and endophilin-dynamin complexes. Introduction into hippocampal neurons of a dominant-negative endophilin construct, which constitutively binds to Ca^{2+} channels, significantly reduces endocytosis-mediated uptake of FM 4-64 dye without abolishing exocytosis. These results suggest an important role for Ca^{2+} channels in coordinating synaptic vesicle recycling by directly coupling to both exocytotic and endocytic machineries.

Introduction

Clathrin-mediated endocytosis is one of the primary mechanisms by which eukaryotic cells internalize nutrients, antigens, and growth factors and recycle receptors and vesicles (Conner and Schmid, 2003; Di Fiore and De Camilli, 2001). At the nerve terminal, clathrin-mediated endocytosis plays a crucial role in synaptic vesicle (SV) recycling (Brodin et al., 2000; Higgins and McMahon, 2002; Murthy and De Camilli, 2003; Takei and Haucke, 2001). Many components of the clathrin-mediated endocytosis machinery have been identified, including dynamin, endophilin, and synaptojanin (Huttner and Schmidt, 2002; Slepnev and De Camilli, 2000). Endophilin has been implicated in several stages of clathrin-mediated SV endocytosis, from generating membrane curvature, an early step, to later events such as vesicle fission and uncoating (Gad et al., 2000; Huttner and Schmidt, 2002; Ringstad et al., 1999; Slepnev and De Camilli, 2000). It displays lysophosphatidic acid acyltransferase activity at its N terminus (Schmidt et al., 1999). Its C-terminal Src-homology-3 (SH3) domain selectively interacts with other endocytic proteins, such as dynamin, and may serve to recruit these proteins to the nerve terminal (Ringstad et al., 1997; Schmidt et al., 1999). Studies have shown that the clathrin-mediated endocytosis machinery, particularly endophilin, is enriched in the release zone, even in unstimulated nerve terminals (Gonzalez-Gaitan and Jackle, 1997; Guichet et al., 2002; Ringstad et al., 2001; Roos and Kelly, 1999; Teng and Wilkinson, 2000). It remains unclear how the universal clathrin-mediated endocytosis machinery can be selectively targeted to release zones, where it is needed after SV exocytosis.

Compared with exocytosis, the exact role of Ca^{2+} in SV endocytosis is not well understood. Mounting evidence suggests that Ca^{2+} is involved in regulating the SV endocytosis process. For instance, retrieval of synaptic membrane at the *Drosophila* neuromuscular junction is Ca^{2+} dependent (Kuromi and Kidokoro, 2002; Ramaswami et al., 1994). Elevated Ca^{2+} levels activate a rapid mode of endocytosis in hippocampal neurons, cochlear inner hair cells, retinal bipolar cells, and chromaffin cells (Beutner et al., 2001; Griesinger et al., 2002; Klingauf et al., 1998; Neher and Zucker, 1993; Neves et al., 2001; Sankaranarayanan and Ryan, 2001). It remains unclear as to how and where Ca^{2+} could exert its regulatory effects.

Through their interaction with the SNARE protein complex, voltage-gated Ca^{2+} channels (VGCCs) are an integral part of the SV release machinery (Catterall, 1999). Ca^{2+} influx through VGCCs plays a key role in regulating fast SV exocytosis (Augustine, 2001; Catterall, 1999; Gundelfinger et al., 2003; Rizo and Sudhof, 2002). Binding of Ca^{2+} to the C2 domain in synaptotagmin serves as the Ca^{2+} sensor to regulate exocytosis (Augustine, 2001; Fernandez-Chacon et al., 2001; Yoshihara et al., 2003). At the nerve terminal, the exocytotic and endocytic processes are tightly coupled and highly coordinated (Gundelfinger et al., 2003). But, the exact mechanisms for such coupling and coordination are poorly understood.

Here, we report that VGCCs are also an important part of the SV endocytic machinery. VGCCs and endophilin form a macromolecular complex in neurons, and formation of this complex is Ca^{2+} dependent. Binding of endophilin to Ca^{2+} channels reaches a maximum at 100–300 nM Ca^{2+}, equivalent to resting Ca^{2+} levels in neurons. When Ca^{2+} exceeds 1 μM, the complex dissociates. Through mutagenesis, we have identified the primary Ca^{2+} binding domain for regulating formation of both endophilin-Ca^{2+} channel and endophilin-dynamin complexes. Finally, transfection into hippocampal neurons of a dominant-negative construct, which displaces the endogenous endophilin from binding to Ca^{2+} channels, significantly reduces uptake of fluorescent dye FM 4-64. The reduction seems to be due primarily to impaired endocytosis. Our results suggest an important

*Correspondence: jfzhang@pharm.med.upenn.edu

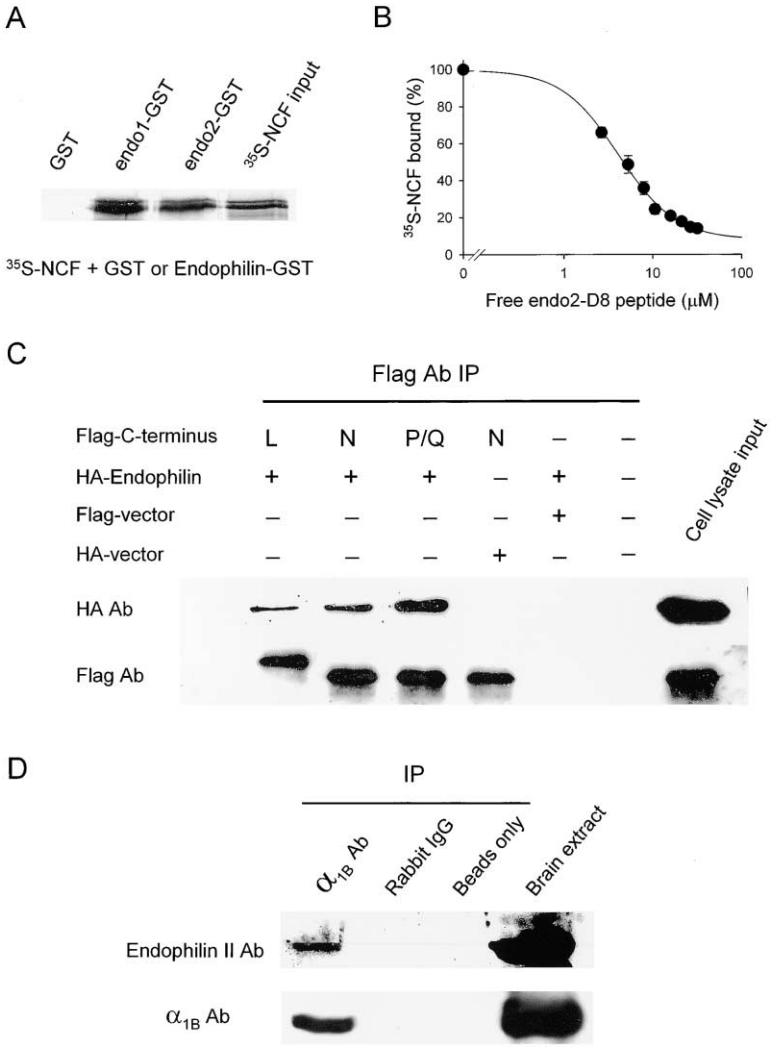

Figure 1. Association of Endophilin with Voltage-Gated Ca^{2+} Channels

(A) GST-fusion protein pulldown assays. Experiments were performed in the presence of 100 nM Ca^{2+}.

(B) Quantitative analysis of competition for endo2 binding to NCF by endo2-D8. Data were normalized to the binding in the absence of endo2-D8 and fitted to an equation: $y = B_{min} + (B_{max} - B_{min})/(1 + (x/IC_{50})^n)$. $IC_{50} = 4.2 \pm 0.48$ μM (mean ± sem, n = 4). Hill coefficient = 1.4 ± 0.08. Experiments were performed in the presence of 300 nM Ca^{2+}. Error bars, if not visible, are within the symbols.

(C) Endophilin interacts with all three types of Ca^{2+} channels. HA-tagged endo2 and Flag-tagged channel C termini were coexpressed in HEK 293 cells. The calculated molecular weights are 73 kDa, 69 kDa, and 68 kDa for L-, N-, and P/Q-type channel C termini respectively. Only the N-type channel C terminus was shown in the input lane.

(D) Formation of the endophilin-Ca^{2+} channel complex in vivo. Brain lysate was immunoprecipitated with an anti-α_{1B} antibody and blots were detected with antibodies against endophilin II and N-type Ca^{2+} channels (α_{1B}). CoIP assays were performed in the absence of Ca^{2+}.

role of VGCCs in coupling exocytotic and endocytic machineries for SV recycling.

Results

Formation of an Endophilin-Ca^{2+} Channel Complex in Neurons

To identify proteins that might interact with Ca^{2+} channels and play a role in Ca^{2+}-dependent signal transduction, we carried out yeast two-hybrid screening of a rat brain cDNA library using the full length C termini of three different Ca^{2+} channel α_1-subunits, α_{1A} (P/Q-type), α_{1B} (N-type), and α_{1C} (L-type), as baits (Maeno-Hikichi et al., 2003). One clone, N427, pulled out by the N-type Ca^{2+} channel C terminus (NCF), encoded a partial sequence of endophilin II (endo2), a member of the endophilin family (Ringstad et al., 1997). The interaction between endo2 and NCF was rigorously tested by several different approaches. In yeast, the interaction was established by both *LacZ* reporter gene assay and galactose-dependent growth in leucine-deficient medium. Binding of endo2 to NCF was verified by GST-fusion protein pulldown assays (Figure 1A). The interaction was further confirmed by coimmunoprecipitation (coIP) assays (Figure 1C). Reciprocal coIP yielded the same results (not shown). Competition studies were carried out using ^{35}S-NCF and endo2-GST in the presence of free endo2-D8, a minimal peptide required for interacting with Ca^{2+} channels (Figure 3). Endo2-D8 competitively inhibited binding of endo2 to NCF. The results were consistent with a one-to-one binding model (Figure 1B).

At least three isoforms of endophilin have been identified, endophilin I (endo1), endophilin II, and endophilin III. Both endo1 and endo2 are primarily expressed in the brain (Ringstad et al., 1997). Pulldown assays showed that both could interact with NCF (Figure 1A). Therefore, in the rest of the paper, we refer to the interaction as between endophilin and Ca^{2+} channels, even though most of the data were collected using endo2 and its mutants. Multiple types of Ca^{2+} channels coexist in neurons, including L-, N-, and P/Q-types (Catterall, 1998; Dunlap et al., 1995; Zhang et al., 1993). In addition to N-type, L- and P/Q-type Ca^{2+} channel C termini could also bind to endophilin (Figure 1C).

Previous studies have demonstrated that endophilin is enriched at the presynaptic nerve terminal, where Ca^{2+} channels are known to be present (Huttner and

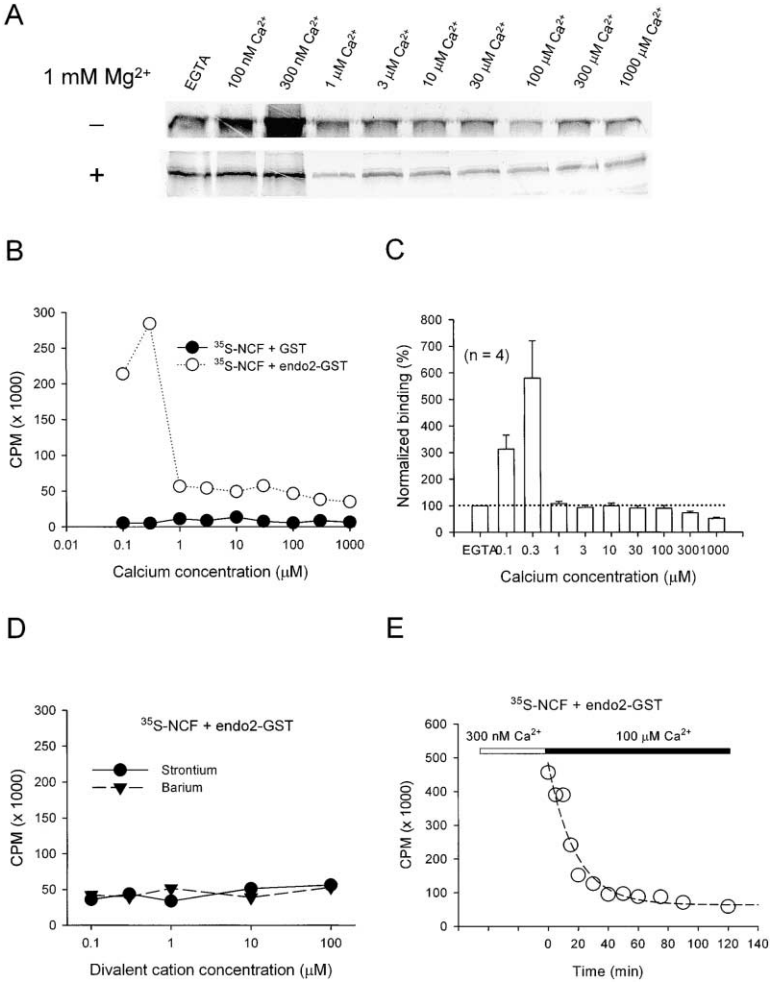

Figure 2. Ca^{2+}-Dependent Formation of the Endophilin-Ca^{2+} Channel Complex

(A) GST-fusion protein pulldown assays performed at different Ca^{2+} concentrations, ranging from 0 (in the presence of 1 mM EGTA) to 1 mM, in the presence or absence of 1 mM Mg^{2+}.

(B) Quantification of the effect of Ca^{2+} on endophilin-Ca^{2+} channel complex. Non-specific binding was trivial and independent of Ca^{2+} (filled circles and solid line).

(C) Summary of the effects of Ca^{2+} on the endophilin-Ca^{2+} channel interaction. Data were normalized to that of 0 Ca^{2+}.

(D) Effects of other divalent cations on the interaction between endophilin and Ca^{2+} channels.

(E) Dissociation kinetics of the endophilin-channel complex at high Ca^{2+}. GST-fused endo2 was incubated with ^{35}S-NCF in a buffer containing 300 nM Ca^{2+} at 4°C overnight. Once the free ^{35}S-NCF was washed off, the endophilin-channel complex was resuspended in a buffer with 100 μM Ca^{2+} (at time 0) and incubated at 4°C for various length of time. The complex was washed again and the radioactivity bound to the GST beads was measured by a scintillation counter. The dash line represents fitting of the data to a single exponential decay function, which yielded a time constant of 18.2 min.

Schmidt, 2002; Slepnev and De Camilli, 2000). To directly demonstrate the existence of the endophilin-Ca^{2+} channel complex, coIP was carried out using lysate prepared from adult rat brain. In agreement with the in vitro data, anti-α_{1B} antibody was able to precipitate endo2 from the crude membrane fraction of the brain preparation (Figure 1D). These results, together with mutagenesis and functional studies (e.g., Figures 3, 6, and 7), suggest that endophilin and Ca^{2+} channels form a complex in vivo.

Effects of Ca^{2+} on Formation of the Endophilin-Ca^{2+} Channel Complex

At the nerve terminal, the resting Ca^{2+} level is approximately 100 nM (Llinas et al., 1992). When VGCCs are activated by the action potential, the local Ca^{2+} concentration can reach as high as 200–300 μM. To test whether dynamic changes in local Ca^{2+} concentrations might affect formation of the endophilin-Ca^{2+} channel complex, pulldown assays were performed at different Ca^{2+} concentrations in the absence or presence of 1 mM Mg^{2+}, another major divalent cation in the cell. The free intracellular Mg^{2+} concentration is 0.5–1 mM in neurons (Brocard et al., 1993).

Ca^{2+} had dramatic effects on the endophilin-channel interaction (Figure 2). First, in the absence of Mg^{2+}, the effect of Ca^{2+} was biphasic (Figures 2A and 2B). Binding of endophilin to Ca^{2+} channels was enhanced by over 3-fold as Ca^{2+} concentration was raised from 0 to 100 nM (Figure 2C). The optimal Ca^{2+} concentration for formation of the endophilin-Ca^{2+} channel complex was near 100–300 nM (Figure 2C). When Ca^{2+} was 1 μM or higher, the endophilin-Ca^{2+} channel complex was significantly reduced. At 1 μM Ca^{2+}, the normalized binding was decreased from 579.86 ± 140.74% to 108.14 ± 8.25% ($n = 4$, $p < 0.02$). When the Ca^{2+} concentration reached 100 μM, the difference was further increased to 6.4-fold (579.86 ± 140.74% versus 90.60 ± 10.03%, $n = 4$, $p < 0.02$).

Second, the association and subsequent dissociation of the endophilin-Ca^{2+} channel complex displayed very steep Ca^{2+} dependency. When the Ca^{2+} concentration was increased from 300 nM to 1 μM (within a half log unit), for instance, the dissociation was already near completion (Figure 2C). The biphasic Ca^{2+} effects and the steepness of Ca^{2+} dependency suggest that multiple Ca^{2+} binding sites may be involved in regulating formation of the endophilin-Ca^{2+} channel complex. In the presence of 1 mM Mg^{2+}, the Ca^{2+}-dependent association of endophilin and Ca^{2+} channels disappeared, whereas the steep Ca^{2+}-dependent dissociation of the endophilin-channel complex remained the same (Figure 2A). These

data suggest that there are at least two distinct Ca^{2+} binding sites, one of which is also sensitive to Mg^{2+}. Both endo1 and endo2 exhibited similar Ca^{2+}-dependent interactions with Ca^{2+} channels (not shown).

Pulldown assays were performed in the presence of strontium or barium instead of Ca^{2+} to further test whether other divalent cations elicited effects similar to Ca^{2+}. Neither Sr^{2+} nor Ba^{2+} affected the interaction between endophilin and NCF (Figure 2D), suggesting that Ca^{2+} plays a major role in regulating the formation of the endophilin-Ca^{2+} channel complex.

We next tested whether the endophilin-channel complex, once formed, could disassemble at high Ca^{2+} levels. The endophilin-channel complex, formed at 300 nM Ca^{2+}, was incubated in a buffer with 100 μM Ca^{2+} for various periods of time at 4°C. As expected, once in the high Ca^{2+} solution, the endophilin-channel complex started to dissociate with time, following a single exponential decay function (Figure 2E). This data suggests that formation of the endophilin-channel complex is readily reversible at high Ca^{2+} concentrations.

Ca^{2+} Channel Binding Domain on Endophilin

Endophilin interacts with its partner proteins through the C-terminal SH3 domain (Huttner and Schmidt, 2000; Slepnev and De Camilli, 2000). To delineate the Ca^{2+} channel binding domain on endophilin, we generated a series of endophilin deletion mutants (Figure 3A). The isolated SH3 domain (D6) failed to pull down ^{35}S-NCF (Figure 3A), indicating that the SH3 domain itself did not interact directly with Ca^{2+} channels. The first 120 amino acid residues (D3) also did not bind to the channel C terminus.

Analysis of the mutants revealed a pattern. Mutants lacking the SH3 domain exhibited much stronger association with the Ca^{2+} channel C terminus compared with those with an intact SH3 domain (Figures 3A and 3B). For instance, removing the SH3 domain from D1 caused a 3-fold increase in binding for D5, from 56,820 ± 2,846 ($n = 3$) to 167,055 ± 16,830 ($n = 6$, $p < 0.01$). The increased affinity between SH3-less mutants and NCF was observed at all Ca^{2+} concentrations tested (Figure 3C). Thus, while the SH3 domain itself did not directly contribute to the formation of the endophilin-Ca^{2+} channel complex, the presence of the SH3 domain appeared to hinder the interaction between endophilin and Ca^{2+} channels. Amino acid residues 200–219 were crucial for the formation of the endophilin-Ca^{2+} channel complex. Inclusion of this segment led to a 7-fold increase in the endophilin-Ca^{2+} channel complex (Figures 3A and 3B). This segment is highly conserved among the three endophilin isoforms (Ringstad et al., 1997).

Ca^{2+}-Dependent Blockade of the Endophilin-Channel Interaction by the SH3 Domain

Two well-defined Ca^{2+} binding domains, the C2 domain and EF-hand, are known to participate in many Ca^{2+}-dependent signaling processes. Although endophilin does not contain any known Ca^{2+} binding domains, the Ca^{2+} channel C terminus has an EF-hand (Babitch, 1990). To determine if this EF-hand was responsible for the Ca^{2+}-dependent formation of the endophilin-channel complex, a mutant was generated with the entire

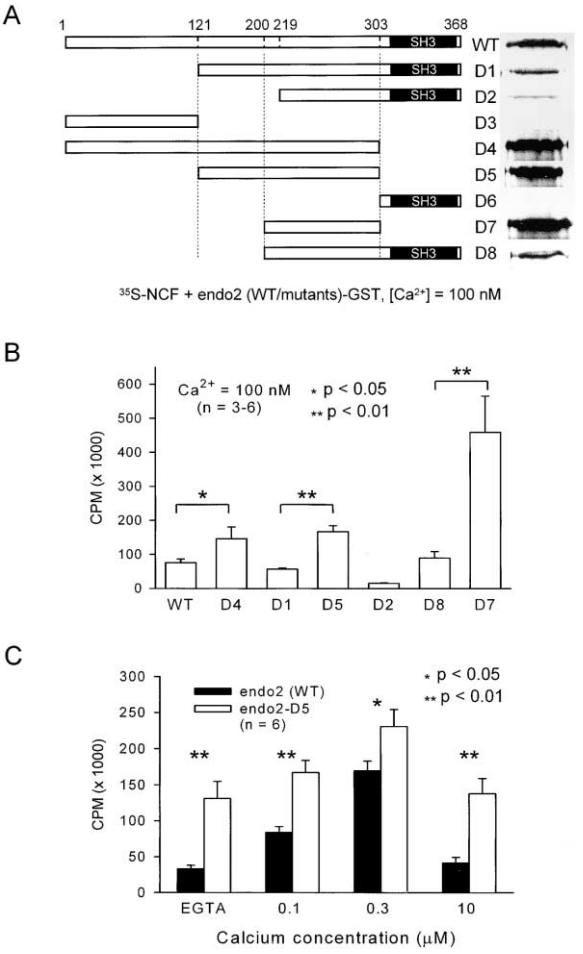

Figure 3. Identification of the Ca^{2+} Channel Binding Domain in Endophilin

(A) Effects of deletion mutations on the interaction between endophilin and the Ca^{2+} channel C terminus. Schematic representation of the wild-type endophilin II and deletion mutants. Numbers represented the starting and ending amino acids for a particular construct.
(B) Deletion of the SH3 domain increases binding of endophilin mutants to Ca^{2+} channels.
(C) SH3-less mutants display increased binding to Ca^{2+} channels at all Ca^{2+} levels.

EF-hand deleted. Removing this EF-hand did not affect the Ca^{2+}-dependent interaction (Figure 4A).

Since endophilin mutants with or without the SH3 domain showed distinct binding to NCF (Figure 3), we examined whether these two groups of mutants exhibited differential sensitivities to Ca^{2+} in their interactions with Ca^{2+} channels. The effects of Ca^{2+} were compared between three pairs of constructs, including WT endo2 versus D4, D1 versus D5, and D8 versus D7 (Figure 3A). All three pairs displayed the same patterns in their binding to NCF at different Ca^{2+} levels. Those with the SH3 domain exhibited robust Ca^{2+}-dependent interactions, in sharp contrast to those without the SH3 domain (Figure 4B). For example, when the Ca^{2+} level was increased from 300 nM to 10 μM, the normalized binding of D8 to NCF was significantly reduced, from 1,568.8 ± 264.0% to 90.9 ± 7.8% ($n = 3$, $p < 0.01$, Figure 4C). D7, on the other hand, remained bound to the channel C terminus even at 1 mM Ca^{2+} (Figures 4B and 4C).

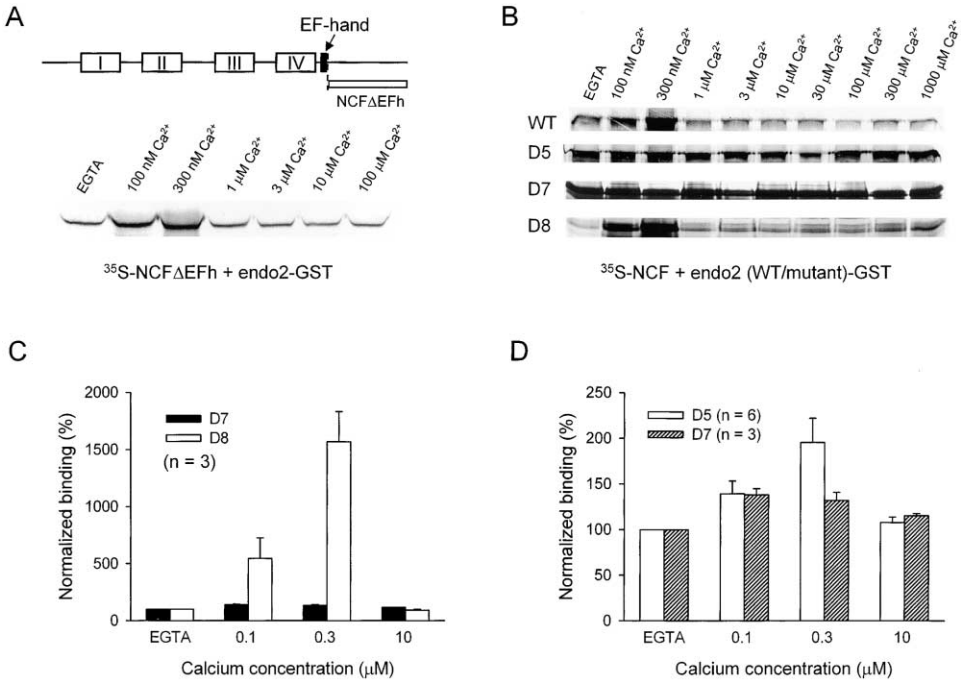

Figure 4. The SH3 Domain Blocks the Interaction between Endophilin and Ca^{2+} Channels

(A) An EF-hand in the Ca^{2+} channel C terminus is not the primary Ca^{2+} binding site for regulating the endophilin-Ca^{2+} channel complex.

(B) Deletion mutants lacking the SH3 domain become insensitive to Ca^{2+} in their interactions with Ca^{2+} channels.

(C) Quantitative comparison between deletion mutants D7 and D8 in their interaction with ^{35}S-NCF at different Ca^{2+} concentrations. Data were normalized to that at 0 Ca^{2+}.

(D) Quantitative comparison between deletion mutants D5 and D7. Compared to D7, D5 displayed a small, but significant, degree of Ca^{2+}-dependent dissociation.

There were some subtle differences among these SH3-less mutants in their Ca^{2+}-dependent binding to NCF. For instance, D5 exhibited some degree of Ca^{2+}-dependent dissociation from NCF (Figure 4D). As the Ca^{2+} level was raised from 300 nM to 10 μM, the normalized binding was decreased from 195.4 ± 26.5% to 107.7 ± 6.1% ($n = 6$, $p < 0.01$). D7, on the other hand, did not show any significant Ca^{2+}-dependent dissociation.

While the SH3 domain itself did not bind directly to Ca^{2+} channels (Figure 3A), the presence of the SH3 domain weakened the interaction between endophilin and Ca^{2+} channels at Ca^{2+} concentrations over 1 μM. One possibility is that at high Ca^{2+} levels, the SH3 domain might interact with another domain within endophilin, consequently preventing the formation of the endophilin-Ca^{2+} channel complex. The prediction from such a hypothesis was that the interaction between the SH3-less mutants and NCF should become sensitive to Ca^{2+} in the presence of a separate SH3 domain peptide. Consistent with this prediction, interaction between ^{35}S-NCF and D7 became Ca^{2+} dependent in the presence of a poly-histidine-tagged SH3 domain peptide (8 μM, Figure 5A). The results suggest that the SH3 domain blocks the formation of endophilin-Ca^{2+} channel complex when the Ca^{2+} level is over 1 μM.

Molecular Nature of the Primary Ca^{2+} Binding Domain

SH3 domains serve as molecular modules for protein-protein interactions, with proline-rich domains (PxxP, PRD) as their partner modules (Pawson, 1995). In addition to the SH3 domain, all endophilins have a PRD (Sparks et al., 1996), located within the Ca^{2+} channel binding domain (amino acid residues 257–264 in endo2, Figure 5B). To test whether this PRD directly interacted with the SH3 domain, a PRD peptide was synthesized and included in the pulldown assay buffer at a final concentration of 10 μM. In the presence of this peptide, the endophilin-channel interaction became insensitive to Ca^{2+} (Figure 5B), as though the SH3 domain were deleted (c.f. Figure 4B). A control peptide with prolines replaced by alanines had no effect (Figure 5B).

To directly demonstrate that the SH3 domain interacted with the PRD, pulldown assays were carried out using the GST-fused SH3 domain (D6, Figure 3A) and the GFP-tagged SH3-less mutants expressed in HEK 293 cells. At low Ca^{2+} levels (0–300 nM), binding of the SH3 domain to D4 was weak (Figure 5C). However, when the Ca^{2+} level was raised to above 1 μM, there was a robust interaction between the SH3 domain and GFP-tagged D4, suggesting that the affinity of the PRD for the SH3 domain is increased by Ca^{2+}. This is opposite to the effects of Ca^{2+} on the endophilin-Ca^{2+} channel interaction (c.f. Figure 2A). Similar results were observed between the SH3 domain and GFP-tagged D7 (not shown). It remains to be determined whether the interaction between the PRD and the SH3 domain is intramolecular or intermolecular, although studies have shown that such an interaction can be intramolecular (Sicheri et al., 1997; Xu et al., 1997).

How does Ca^{2+} alter the affinity of the PRD for the

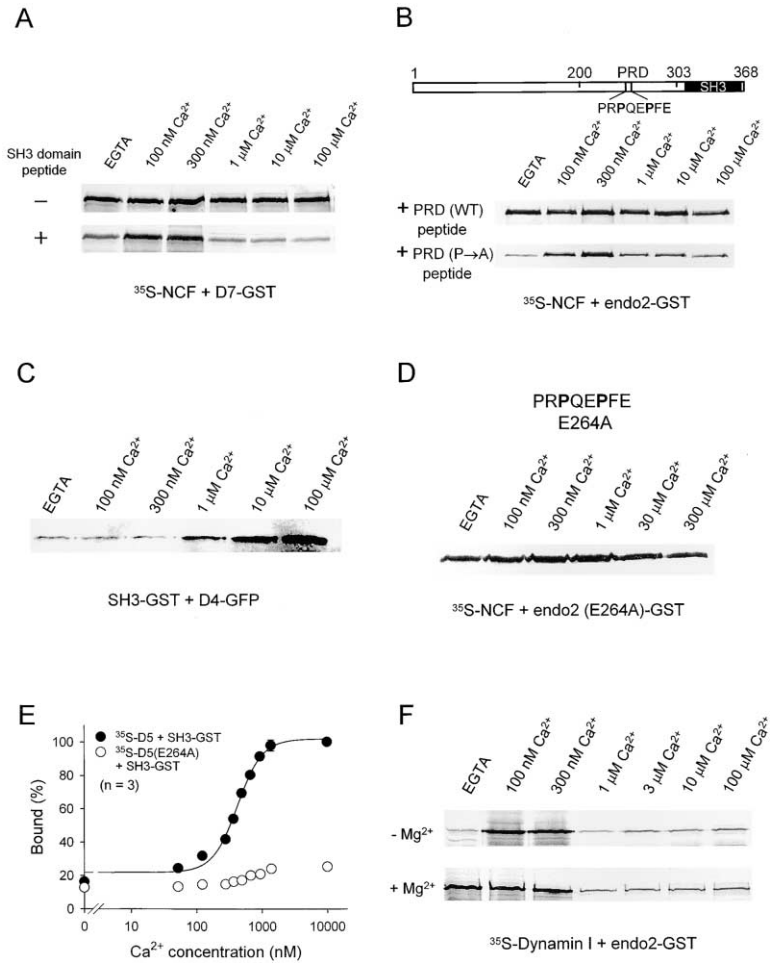

Figure 5. Ca^{2+}-Dependent Change in the Affinity of the PRD for the SH3 Domain within Endophilin

(A) SH3 domain peptide (final concentration 8 μM) restores the Ca^{2+}-dependent interaction between SH3-less endophilin mutants and the Ca^{2+} channel C terminus.

(B) Effects of the PRD peptide on the interaction between endophilin and NCF. A diagram depicts the location of the PRD within the endophilin molecule. Pulldown assays were performed in the presence of a synthetic peptide, PRD (WT), encompassing the proline rich domain: PRREFKPRPQEPFELG. A peptide with prolines replaced by alanines, PRD (P → A), was used as the control.

(C) Ca^{2+}-dependent interaction between the SH3 domain and SH3-less endophilin mutants. An anti-GFP antibody was used for immunoblotting.

(D) An E264A point mutation eliminates the Ca^{2+}-dependent interaction between endophilin and the Ca^{2+} channel C terminus.

(E) Dose-response relationship for Ca^{2+} to increase binding of the PRD and the SH3 domain. Pulldown assays were carried out using ^{35}S-labeled D5 or D5 (E264A) and GST-fused SH3 domain (D6). Equal amounts of D5 (WT) or D5 (E264A) were used. The radioactivity bound to GST beads was measured by a scintillation counter. All data were normalized to that of wild-type D5 at 10 μM Ca^{2+}. For wild-type D5, data were fitted to a dose-response equation: $y = B_{min} + (B_{max} - B_{min})*x^n/(x^n + Kd^n)$, which yielded a Kd for Ca^{2+} of 425.2 ± 21.3 nM and a Hill coefficient of 2.3 ± 0.09 (mean ± sem). Error bars, if not seen, are within the symbols. We did not fit the data of D5 (E264A), since the binding might not reach saturation at this Ca^{2+} range.

(F) Dynamin-endophilin interaction is also sensitive to Ca^{2+}. All results shown in this figure are representatives of at least three separate experiments.

SH3 domain? Depending on their orientations, proline-rich domains can be divided into two classes, class I and class II (Mayer, 2001; Pawson, 1995). The PRD in endo2 resembles that of class II, which bears the signature sequence of **PxxPx**+, where + denotes a basic residue, typically an arginine (Mayer, 2001; Tong et al., 2002). This basic residue is thought to determine the affinity and specificity of a PRD to its SH3 domain by binding to a negatively charged pocket on the SH3 domain (Nguyen et al., 1998; Pawson, 1995). The PRD in endo2, however, deviates from this consensus sequence in that it has a negatively charged glutamate residue in this key position: PR**PQEPFE** (E264). Furthermore, there are additional negative charges in the immediate vicinity of the core **PxxP** sequence. Such multiple negative charges are rarely seen in other class II proline-rich domains (Tong et al., 2002). For a typical class II PRD, introduction of a negative charge immediately after the **PxxP** core sequence abolishes its affinity for the SH3 domain (Zhao et al., 2000).

On the other hand, glutamate residues are known to play a key role in forming Ca^{2+} binding domains, such as the EF-hand. Often, multiple glutamate residues are required to form a high-affinity binding site for Ca^{2+}. Examples include the Ca^{2+} selectivity filter in Ca^{2+} channels, where four glutamate residues in the Ca^{2+} channel pore region form a high-affinity Ca^{2+} binding site with the Kd for Ca^{2+} of 1 μM (Yang et al., 1993). We hypothesized that E264 might be part of a Ca^{2+} binding site and that binding of Ca^{2+} to E264 could increase the affinity of the PRD for the SH3 domain in endophilin.

To test this hypothesis, a point mutation was generated in which glutamate 264 was replaced with alanine (endo2 E264A). Binding of the E264A mutant to NCF became insensitive to Ca^{2+} (Figure 5D), as though the SH3 domain had been deleted (c.f. Figure 4B). The results suggested that E264 is part of the Ca^{2+} binding site(s). The importance of E264 was further evaluated by pulldown assays using ^{35}S-labeled D5 (WT) or D5 (E264A) and the GST-fused SH3 domain. As expected, binding of D5 to the SH3 domain increased with Ca^{2+} (Figure 5E). The increase was over 6-fold when Ca^{2+} was increased from 0 to 10 μM. Fitting the data with a dose-response curve yielded the Kd for Ca^{2+} of 425.2 ± 21.3 nM (n = 3) and the Hill coefficient of 2.3 ± 0.09, indicating that at least two Ca^{2+} ions were associated

with endophilin. The Kd for Ca^{2+} and steep Ca^{2+}-dependent association of the PRD and the SH3 domain resulted in the steep dissociation of the endophilin-channel complex when Ca^{2+} rose from 300 nM to 1 μM (Figure 2). In sharp contrast, the E264A mutation severely hampered binding of the mutant D5 to the SH3 domain, particularly at high Ca^{2+} levels. This led to the failure of the mutant endophilin to dissociate from the channel at high Ca^{2+} levels (Figure 5D). These findings suggest that Ca^{2+} can bind to endophilin directly and that E264 plays a critical role in Ca^{2+}-dependent increase in the affinity between the PRD and the SH3 domain. This glutamate residue is conserved in both endo1 and endo2 (Ringstad et al., 1997). Since multiple glutamate residues are required for formation of a high-affinity Ca^{2+} binding site (e.g.Yang et al., 1993), it remains to be investigated whether other glutamate residues contribute to the formation of the Ca^{2+} binding site(s) in endophilin.

Endophilin interacts with other endocytic proteins, such as dynamin, through its SH3 domain (Huttner and Schmidt, 2002; Slepnev and De Camilli, 2000). The effect of Ca^{2+} on the interaction between the PRD and the SH3 domain within endophilin led us to investigate whether the interaction of endophilin and dynamin was also sensitive to Ca^{2+}. Similar to its effects on the endophilin-channel interaction, Ca^{2+} exerted the steep biphasic effects on the endophilin-dynamin complex in the absence of Mg^{2+}. In the presence of 1 mM Mg^{2+}, the endophilin-dynamin complex only displayed Ca^{2+}-dependent dissociation (Figure 5F).

Endophilin-Ca^{2+} Channel Complex Is Required for Clathrin-Mediated SV Endocytosis

As a first step toward understanding the importance of the endophilin-Ca^{2+} channel complex in SV endocytosis, we sought to determine whether introduction of a dominant-negative endophilin construct into hippocampal neurons could affect SV endocytosis. Based on biochemical studies, we elected to use GFP-tagged D5 (E264A) as the dominant-negative construct (Figure 3A). Because of N- and C-terminal deletions, this construct does not have the acyltransferase activity and will not interact with other endocytic proteins (Farsad et al., 2001; Guichet et al., 2002; Schmidt et al., 1999; Slepnev and De Camilli, 2000). Other than its interaction with Ca^{2+} channels (this study), the middle portion of endophilin is not known to interact with any other proteins directly or indirectly involved in synaptic transmission. D5 displayed a much higher affinity for Ca^{2+} channels and the binding was insensitive to Ca^{2+} (Figures 3 and 4). Hence, the mutant should bind selectively to Ca^{2+} channels. In addition, the E264A mutation eliminated the possibility of its interaction with endogenous endophilin through the PRD (Figure 5E). Preliminary tests showed that expression of GFP-tagged D5 (E264A) was much better than D7 (E264A) in hippocampal neurons. Thus, introduction of D5 (E264A) into hippocampal neurons should compete with the endogenous endophilin for association with Ca^{2+} channels but would not carry out any biological functions. Transient expression of D5 (E264A) in hippocampal neurons did not affect formation of functional synapses, as revealed by immunostaining of synapsin, a presynaptic protein (Figure 6A), and by electrophysiology recordings (Figure 7).

We hypothesized that interaction of endophilin with Ca^{2+} channels could recruit endophilin to the release zone. A simple prediction is that overexpression of D5 (E264A) would displace the endogenous endophilin at the release zone, thus impairing the clathrin-mediated SV endocytosis. To test this prediction, we performed FM 4-64 dye uptake experiments on cultured hippocampal neurons transfected with GFP, endo2-GFP, or D5-GFP (E264A). FM 4-64 is a derivative of FM 1-43, a fluorescent dye which becomes trapped in SVs after endocytosis (Betz and Bewick, 1993). FM dye was loaded into synaptic vesicles by depolarizing neurons with a 40 mM K^+ solution. For neurons transfected with GFP or GFP-tagged endophilin, uptake of FM 4-64 (red puncta) was found throughout the GFP-labeled axons (Figure 6B). In contrast, neurons transfected with D5 (E264A) often displayed long segments of axons devoid of FM 4-64 staining. Quantitative analysis showed that the intensity of FM 4-64 staining was significantly reduced (Figure 6C), indicating that SV endocytosis process might be impaired as a result of overexpression of D5 (E264A).

Electrophysiology recordings were performed to investigate whether reduction of the FM4-64 uptake by D5 (E264A) resulted from impaired endocytosis or the arrest of exocytosis. Evoked excitatory postsynaptic currents (EPSCs) were recorded, by dual whole-cell recordings, from neurons whose presynaptic neurons were transfected with wild-type endophilin or D5 (E264A). Neurons transfected with either construct were capable of releasing neurotransmitters in response to brief depolarizing pulses (Figures 7A and 7B). At low frequency stimulations (0.1 Hz), the EPSC amplitude in D5 (E264A)-transfected neurons was 500.1 $\pm$ 154.6 pA ($n = 20$), which was slightly reduced but not significantly different from that of neurons transfected with WT endophilin (818.2 $\pm$ 221.6 pA, $n = 12$; $p > 0.2$; Figure 7E). The results suggested that D5 does not significantly affect SV exocytosis. Ablation of endophilin in *Drosophila* yielded similar results (Verstreken et al., 2002). Analysis of spontaneous miniature EPSCs (mEPSCs) showed that transfection of D5 (E264A) did not alter either the mEPSC amplitude (23.2 $\pm$ 2.1 pA for D5, $n = 11$; 24.5 $\pm$ 1.4 for WT, $n = 9$; $p > 0.6$) or the mEPSC frequency (1.34 $\pm$ 0.28 for D5, $n = 11$; 1.88 $\pm$ 0.44 for WT, $n = 9$; $p > 0.3$; Figures 7C, 7D, 7F, and 7G). These results indicated that D5 (E264A) did not change the postsynaptic receptor properties.

The effects of D5 (E264A) were further evaluated by high frequency stimulations to produce short-term synaptic depression as a result of depletion of the readily releasable pool of synaptic vesicles (RRP). If the primary effect of D5 (E264A) was to impair SV endocytosis as suggested by the imaging studies (Figure 6), we would expect that at high frequency stimulations, short-term synaptic depression would become more profound due to impaired endocytosis in neurons transfected with D5 (E264A). To test this hypothesis, transfected neurons were repetitively stimulated at 5 Hz (100 stimuli). As expected, the EPSC amplitude in neurons transfected with D5 (E264A) ($n = 7$) decreased quickly and reached a significantly lower plateau ($\sim$20% of the control) com-

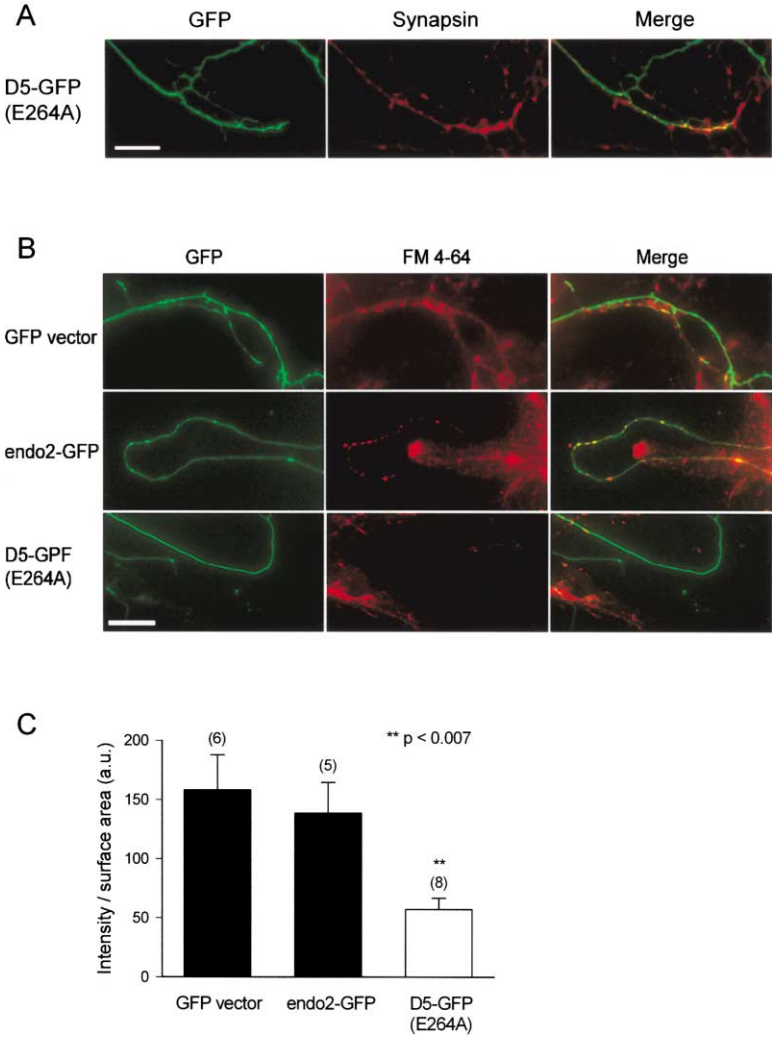

Figure 6. A Dominant-Negative Endophilin Construct Reduces Uptake of FM4-64 in Presynaptic Boutons

(A) Immunostaining of a presynaptic protein, synapsin, in D5 (E264A)-transfected neurons. Scale bar = 25 μm.

(B) Effect of D5 (E264A) on FM 4-64 uptake. Scale bar = 25 μm.

(C) Summary of FM 4-64 uptake for neurons transfected with GFP, endo2-GFP, and D5-GFP (E264A). Numbers in parentheses represent that of transfected neurons of at least three batches of transfection. One way ANOVA was used for group comparison among three different conditions.

pared to that in neurons transfected with WT endophilin ($n = 5$, $p < 0.001$ for the last 5 points, Figure 7H), consistent with previous observations when SV endocytosis was impaired (Shupliakov et al., 1997; Verstreken et al., 2002).

When given multiple train stimulations, there was a steady decrease in the average EPSC amplitude evoked at 0.1 Hz during the interval between train stimulations (Figure 7I). Again, neurons transfected with D5 (E264A) ($n = 6$) exhibited an accelerated decrease in the EPSC amplitude compared to that in neurons transfected with WT endophilin ($n = 5$) (Figure 7I, $p < 0.05$ after the 2nd and 3rd train, and $p < 0.002$ after 4th train). The difference in EPSC amplitudes after train stimulations suggested that replenishment of the RRP is hindered in the D5-transfected neurons, most likely as a consequence of impaired SV endocytosis. Overall, results from imaging and electrophysiology demonstrated that the effects of the dominant-negative construct were primarily on SV endocytosis, consistent with recent reports which showed that ablation of endophilin in *Drosophila* impaired clathrin-mediated vesicle endocytosis (Guichet et al., 2002; Verstreken et al., 2002). We conclude that the endophilin-Ca^{2+} channel complex was critical for clathrin-mediated SV endocytosis.

Discussion

Our results show a direct interaction between VGCCs and the endocytic machinery. We propose that through interactions with endophilin, VGCCs serve as an anchor to recruit the clathrin-mediated endocytosis machinery to the release zone where SV endocytosis is to take place. Such a mechanism is reminiscent of the interaction between VGCCs and the exocytotic machinery (Catterall, 1999) and is consistent with observations that the clathrin-mediated endocytosis machinery is enriched in the release zone (Gonzalez-Gaitan and Jackle, 1997; Ringstad et al., 2001; Roos and Kelly, 1999; Teng and Wilkinson, 2000). Thus, as with exocytosis, VGCCs are also an integral part of the SV endocytic machinery. While the interaction between VGCCs and the exocytotic machinery, such as syntaxin, occurs at the II-III loop of the Ca^{2+} channel α_1 subunit (Sheng et al., 1996), the interaction with the clathrin-mediated endocytosis machinery is through the channel C terminus (current study). Thus, through these interactions, Ca^{2+} channels bring both exocytotic and endocytic machineries in close proximity, providing a potential mechanism for spatial coordination of vesicular exocytosis and endocytosis (Gundelfinger et al., 2003).

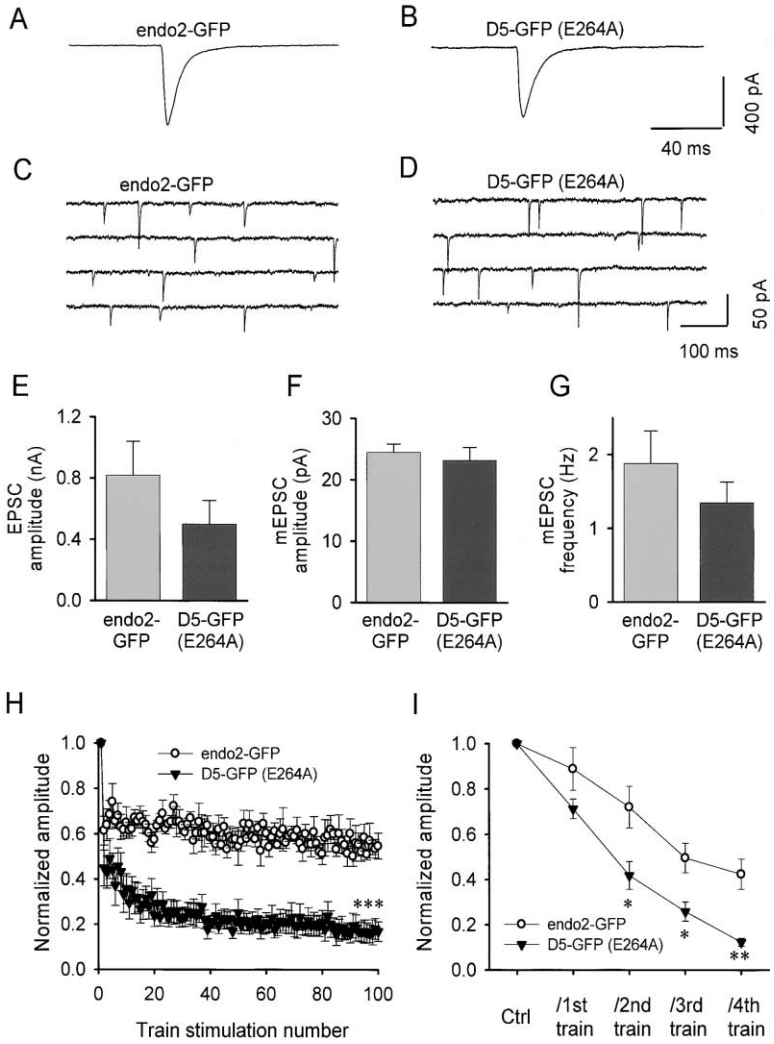

Figure 7. Quantitative Analysis of the Effects of WT and a Dominant-Negative Endophilin Construct on Basal and Sustained Neurotransmitter Release

(A and B) Representative traces of the average EPSCs evoked from a presynaptic neuron transfected with endo2-GFP (A) or D5-GFP (E264A) (B).

(C and D) Typical traces showing mEPSCs in an endo2-GFP transfected neuron (C) and a D5-GFP (E264A) transfected neuron (D).

(E) D5 (E264A) has no significant effect on the EPSC amplitude. EPSCs were recorded from neurons transfected with WT endophilin ($n = 12$) or D5 (E264A) ($n = 20$, $p > 0.2$).

(F and G) D5 (E264A) does not change the mEPSC amplitude ($p > 0.6$) or frequency ($p > 0.3$).

(H) Effects of D5 (E264A) on short-term synaptic depression. Normalized EPSC amplitude during the first train stimulation (5 Hz, 100 stimuli) recorded from neurons transfected with WT endophilin ($n = 5$) or D5 (E264A) ($n = 7$). $p < 0.001$ for the last five points.

(I) Effects of multiple train stimulations on the EPSC amplitude. Multiple train stimulations (5 Hz, 100 stimuli) were applied with a 3-min interval, during which the presynaptic neuron was stimulated at 0.1 Hz. EPSCs recorded during the interval from WT endophilin ($n = 5$) or D5 (E264A) ($n = 6$) transfected neurons were averaged and normalized to that obtained before stimulations. *, $p < 0.05$; **, $p < 0.002$.

It is well established that Ca^{2+} influx through VGCCs is crucial for release of neurotransmitters at the nerve terminal (Augustine, 2001; Catterall, 1999; Gundelfinger et al., 2003; Rizo and Sudhof, 2002). Through their interaction with syntaxin, VGCCs become part of the SNARE protein complex for exocytosis. Syntaxin-Ca^{2+} channel interaction is Ca^{2+}-dependent, presumably responsible for Ca^{2+}-dependent docking of SVs to the release zone (Sheng et al., 1996). Binding of Ca^{2+} to synaptotagmin serves as a trigger for neurotransmitter release (Fernandez-Chacon et al., 2001). The data in this study provide a plausible mechanism by which Ca^{2+} may regulate SV endocytosis (Beutner et al., 2001; Griesinger et al., 2002; Klingauf et al., 1998; Kuromi and Kidokoro, 2002; Neher and Zucker, 1993; Neves et al., 2001; Ramaswami et al., 1994; Sankaranarayanan and Ryan, 2001). Formation of the endophilin-Ca^{2+} channel complex as well as the endophilin-dynamin complex is Ca^{2+}-dependent (Figures 2 and 5). In particular, Ca^{2+}-dependent dissociation of these complexes occurs at the Ca^{2+} concentration range when Ca^{2+} channels are activated by action potentials during triggered exocytosis, allowing Ca^{2+} to regulate SV endocytosis at the beginning of the clathrin-mediated endocytosis process. Thus, Ca^{2+} influx through VGCCs may serve as a signal for temporal coordination of vesicular exocytosis and endocytosis (Gundelfinger et al., 2003).

We have demonstrated a role for the SH3 domain in regulating the interaction between endophilin and its partner proteins, particularly the Ca^{2+}-dependent dissociation of endophilin-Ca^{2+} channel and endophilin-dynamin complexes. The affinity of the PRD to the SH3 domain within endophilin is determined by Ca^{2+}. When the Ca^{2+} level is low, the PRD is not bound to the SH3 domain, allowing binding of endophilin to Ca^{2+} channels and/or dynamin. When the Ca^{2+} concentration rises to above 1 μM, binding of Ca^{2+} to E264 in the PRD significantly increases the affinity of the PRD for the SH3 domain. This, in turn, blocks the access of Ca^{2+} channels and dynamin to endophilin. Thus we propose that this Ca^{2+}-dependent change in the affinity of the PRD for the SH3 domain within endophilin serves as the primary Ca^{2+} sensor for the formation of the endophilin-Ca^{2+} channel and endophilin-dynamin complexes. In addition, our results provide an example that the affinity of the PRD for its SH3 domain can be regulated by physiological factors targeting at amino acid residues in the vicinity of the core **PxxP** signature sequence.

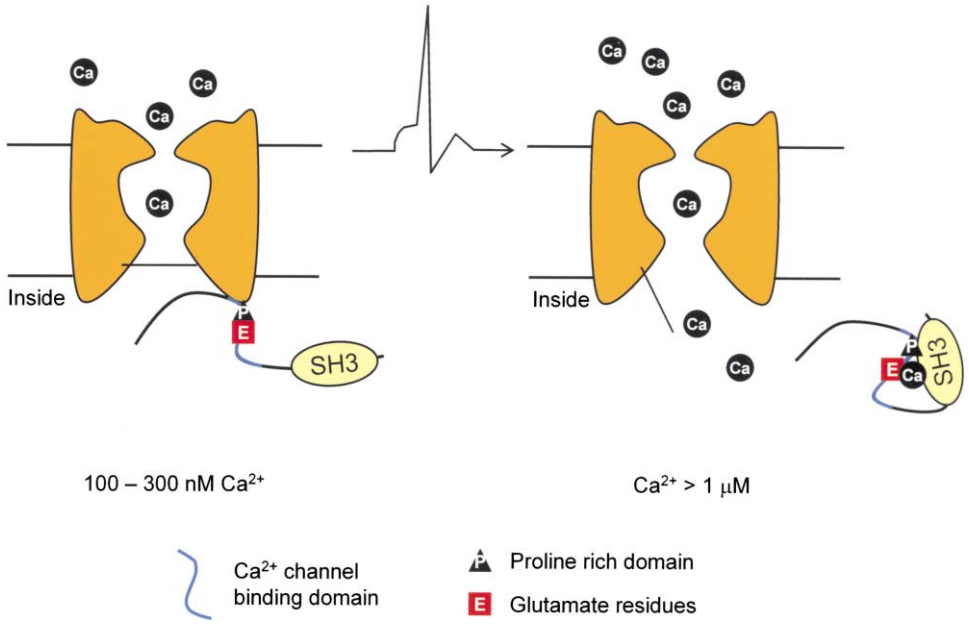

Figure 8. A Molecular Model for Ca^{2+}-Dependent Interaction between Endophilin and Ca^{2+} Channels

The model depicts the interaction between the PRD and its SH3 domain within endophilin as intramolecular, but it is also possible that the interaction could be intermolecular.

We propose that endophilin has two distinct modes or conformations, an open mode and a closed mode (Figure 8). Under resting Ca^{2+} levels (100–300 nM), endophilin is in its open mode due to the low affinity of the PRD for the SH3 domain. In this open mode, endophilin is able to interact with both Ca^{2+} channels and dynamin and the interactions serve to recruit the endocytic machinery into the nerve terminal. When local Ca^{2+} levels rise to over 1 μM as a consequence of activation of VGCCs, binding of Ca^{2+} to E264 in the PRD switches endophilin to the closed mode, when the PRD locks onto the SH3 domain. In this closed mode, endophilin is no longer available for binding to either Ca^{2+} channels or dynamin, which would presumably allow the liberated endophilin and dynamin to become actively involved in endocytosis immediately after SV exocytosis. By coupling tightly to both the exocytotic and endocytic machineries, voltage-gated Ca^{2+} channels are thus uniquely positioned to coordinate the SV recycling process.

Experimental Procedures

Yeast Two-Hybrid Screening

Details of screening can be found elsewhere (Maeno-Hikichi et al., 2003). The C terminus of α_{1A} (CaV2.1, amino acid residues 1819–2422; accession number X57477), α_{1B} (CaV2.2, 1707–2339; M94172), or α_{1C} (CaV1.2, 1505–2171; X15539) subunit was used as bait to screen a rat brain cDNA library (OriGene Inc.). Approximately 7×10^6 to 1×10^8 independent clones were screened for each bait. A total of over 200 clones were sequenced out of approximately 2,000 positive clones.

Construction and Expression of Recombinant Proteins

The PCR-based method was used to generate all of the constructs used in this study. Point mutations were introduced with the QuikChange kit (Stratagene). All constructs were verified by sequencing. To generate recombinant proteins, cDNA constructs were subcloned into pGEX-4T-1 (Pharmacia) for GST-fused proteins or pQE-30 (Qiagen) for poly-histidine-tagged (6×His) proteins. GST-fusion proteins and 6×His proteins were produced in *E. coli*. Glutathione agarose beads (Pierce) were used to purify GST-fused proteins. Ni-NTA columns (Qiagen) were used for purification of 6×His proteins. To express the recombinant proteins in mammalian cells, cDNA constructs were subcloned into the following vectors: HA-tagged pcDNA 3, FLAG-tagged pcDNA 3, or pEGFP (Clontech). The calcium phosphate method was used for transfection in HEK 293 cells or hippocampal neurons.

GST-Fusion Protein Pulldown Assays

Pulldown assays were carried out as previously described (Maeno-Hikichi et al., 2003). Briefly, ^{35}S-labeled proteins were synthesized using an in vitro protein translation kit (Promega). The assay buffer contained 100 mM NaCl, 20 mM TrisHCl, and 5% glycerol (pH 7.0) along with 1% Triton X-100 and a cocktail of protease inhibitors (phenylmethylsulfonyl fluoride, 1 μM; pepstatin, 1 μg/ml; leupeptin, 1 μg/ml; aprotinin, 1 μg/ml; and benzamidine, 0.1 mg/ml). Approximately 5 μg of GST-fused protein were incubated with 2 μl of ^{35}S-labeled protein with gentle rocking. The length of incubation varied from 2 hr to overnight. All pulldown assays were performed at 4°C. The results were analyzed by SDS-PAGE and autoradiography or by a scintillation counter. Typically, 0.5 μl of ^{35}S-labeled protein was used as input on the gel. Values of CPM (count per minute) were expressed as mean ± SEM. To minimize the variability of radioactivity between experiments, CPM values were normalized to that obtained in the presence of 1 mM EGTA for quantification of the Ca^{2+} effects. Non-specific binding was insignificant and independent of Ca^{2+} (e.g., Figures 1A and 2B). A computer program was used to prepare Ca^{2+} solutions at low concentrations (http://www.stanford.edu/cpatton/maxc.html).

Coimmunoprecipitation and Immunoblotting

Coimmunoprecipitation of endophilin and calcium channels was performed using adult rat cortical extracts as previously described (Maeno-Hikichi et al., 2003). Briefly, the soluble membrane fraction of adult rat cortical extracts was incubated with anti-α_{1B} antibody (Alomone Labs) conjugated protein G sepharose beads over night at 4°C. The IP buffer contained (in mM): NaCl, 137; KCl, 2.7; Na_2HPO_4, 4.3; KH_2PO_4, 1.4; EGTA, 5; and EDTA 5 (pH 7.5). Immune complexes

were resolved by SDS-PAGE, and analyzed by immunoblotting with antibodies against endophilin II (Santa Cruz) and α_{1B}.

Hippocampal Neuron Culture

Hippocampal neurons were cultured in microislands from postnatal 1- to 2-day-old Sprague-Dawley rats (Bekkers and Stevens, 1991). The culture medium contained MEM, 5% fetal bovine serum, B-27, an additional 20 mM glucose, and 25 unit/ml penicillin/streptomycin supplied with 5% CO_2. Typically, cultured neurons were transfected with different constructs on 10 DIV (days in vitro) and physiology experiments were performed on 12 DIV.

Immunocytochemistry

Hippocampal neurons were fixed with 4% paraformaldehyde and 4% sucrose in PBS for 10 min, permeabilized with 0.25% Triton X-100 in PBS for 5 min, and quenched with 0.1 M glycine in PBS. An anti-synapsin I antibody (1:400, Oncogene) was used for immunostaining. An alexa 568-conjugated secondary antibody (Molecular Probes) was used for visualization. Fluorescent images were collected with a Nikon Eclipse TE200 inverted microscope.

Electrophysiology Recordings and FM 4-64 Labeling

Evoked EPSCs were obtained on cultured hippocampal neurons using dual whole-cell recordings by stimulating transfected presynaptic neurons with brief depolarizing pulses (−70 mV to 0 mV, 1.5 ms). Spontaneous miniature EPSCs were recorded from transfected neurons. A MultiClamp 700A amplifier (dual channels) and pClamp 8 software (Axon Instrument, CA) were used for data acquisition and analysis. mEPSCs were analyzed using MiniAnalysis software (Synaptosoft Inc.). Current traces were digitized at 10 kHz and low-pass filtered at 1 kHz. The extracellular bath solution contained (in mM): NaCl, 128; KCl, 5; $CaCl_2$, 2; $MgCl_2$, 1; glucose, 30; and HEPES, 25 (pH 7.3). The pipette solution contained (in mM): KCl, 147; Na_2-phosphocreatine, 5; EGTA, 2; MgATP, 2; Na_2GTP, 0.3; and HEPES, 10 (pH 7.2).

Imaging experiments were performed on a Zeiss inverted microscope (Axiovert 200) equipped with an ORCA-ER CCD camera (Hamamatsu, Japan) and DG-5 fast wavelength switcher (Sutter Inc., CA). Fluorescence images were acquired and analyzed with Simple PCI imaging software (Compix Inc., Pittsburg), and processed with Photoshop. GFP and FM 4-64 fluorescence signals were obtained using band-pass filters from Chroma (Oregon). Neurons were stained in 10 μM FM 4-64 and 40 mM potassium solution for 2 min. After collecting FM staining images, neurons were subjected to destaining in 40 mM potassium solution for 6 min. Images obtained after destaining were used for background subtraction. The intensity of FM 4-64 fluorescence was quantified by measuring the sum of FM fluorescence intensity on subtracted images (staining minus destaining) along an axon segment delineated by GFP signal. On average, the total length of axon segments measured was 478.6 μm per neuron. Arbitrary units (au) were calculated by dividing the sum of the FM fluorescence intensity by the surface area of the measured axon segment.

Data were expressed as mean ± SEM.

Acknowledgments

We thank I. Levitan, K. Foskett, C. Deutsch, J. Field, J. Eberwine, J. Meinkoth, and R. Pittman for stimulating discussions and helpful suggestions, M. Lemmon and M. Marks for the human dynamin I construct, R. Pittman for the use of the Nikon Eclipse TE200 inverted microscope, and M. Jiang for technical help. This work was supported by grants from the National Institutes of Health (NS39355, J.F.Z.), the American Heart Association (J.F.Z.), the National Alliance for Research on Schizophrenia and Depression (Y.M.H.), and the Pennsylvania State University Life Science Consortium Innovative Biotechnology Research Fund (G.C.).

Received: May 5, 2003
Revised: August 27, 2003
Accepted: August 29, 2003
Published: October 2, 2003

References

Augustine, G.J. (2001). How does calcium trigger neurotransmitter release? Curr. Opin. Neurobiol. *11*, 320–326.

Babitch, J. (1990). Channel hands. Nature *346*, 321–322.

Bekkers, J.M., and Stevens, C.F. (1991). Excitatory and inhibitory autaptic currents in isolated hippocampal neurons maintained in cell culture. Proc. Natl. Acad. Sci. USA *88*, 7834–7838.

Betz, W.J., and Bewick, G.S. (1993). Optical monitoring of transmitter release and synaptic vesicle recycling at the frog neuromuscular junction. J. Physiol. *460*, 287–309.

Beutner, D., Voets, T., Neher, E., and Moser, T. (2001). Calcium dependence of exocytosis and endocytosis at the cochlear inner hair cell afferent synapse. Neuron *29*, 681–690.

Brocard, J.B., Rajdev, S., and Reynolds, I.J. (1993). Glutamate-induced increases in intracellular free Mg^{2+} in cultured cortical neurons. Neuron *11*, 751–757.

Brodin, L., Low, P., and Shupliakov, O. (2000). Sequential steps in clathrin-mediated synaptic vesicle endocytosis. Curr. Opin. Neurobiol. *10*, 312–320.

Catterall, W.A. (1998). Structure and function of neuronal Ca^{2+} channels and their role in neurotransmitter release. Cell Calcium *24*, 307–323.

Catterall, W.A. (1999). Interactions of presynaptic Ca^{2+} channels and SNARE proteins in neurotransmitter release. Ann. N Y Acad. Sci. *868*, 144–159.

Conner, S.D., and Schmid, S.L. (2003). Regulated portals of entry into the cell. Nature *422*, 37–44.

Di Fiore, P.P., and De Camilli, P. (2001). Endocytosis and signaling. an inseparable partnership. Cell *106*, 1–4.

Dunlap, K., Luebke, J.I., and Turner, T.J. (1995). Exocytotic Ca^{2+} channels in mammalian central neurons. Trends Neurosci. *18*, 89–98.

Farsad, K., Ringstad, N., Takei, K., Floyd, S.R., Rose, K., and De Camilli, P. (2001). Generation of high curvature membranes mediated by direct endophilin bilayer interactions. J. Cell Biol. *155*, 193–200.

Fernandez-Chacon, R., Konigstorfer, A., Gerber, S.H., Garcia, J., Matos, M.F., Stevens, C.F., Brose, N., Rizo, J., Rosenmund, C., and Sudhof, T.C. (2001). Synaptotagmin I functions as a calcium regulator of release probability. Nature *410*, 41–49.

Gad, H., Ringstad, N., Low, P., Kjaerulff, O., Gustafsson, J., Wenk, M., Di Paolo, G., Nemoto, Y., Crun, J., Ellisman, M.H., et al. (2000). Fission and uncoating of synaptic clathrin-coated vesicles are perturbed by disruption of interactions with the SH3 domain of endophilin. Neuron *27*, 301–312.

Gonzalez-Gaitan, M., and Jackle, H. (1997). Role of *Drosophila* α-adaptin in presynaptic vesicle recycling. Cell *88*, 767–776.

Griesinger, C.B., Richards, C.D., and Ashmore, J.F. (2002). FM1–43 Reveals Membrane Recycling in Adult Inner Hair Cells of the Mammalian Cochlea. J. Neurosci. *22*, 3939–3952.

Guichet, A., Wucherpfennig, T., Dudu, V., Etter, S., Wilsch-Brauniger, M., Hellwig, A., Gonzalez-Gaitan, M., Huttner, W.B., and Schmidt, A.A. (2002). Essential role of endophilin A in synaptic vesicle budding at the Drosophila neuromuscular junction. EMBO J. *21*, 1661–1672.

Gundelfinger, E.D., Kessels, M.M., and Qualmann, B. (2003). Temporal and spatial coordination of exocytosis and endocytosis. Nat. Rev. Mol. Cell Biol. *4*, 127–139.

Higgins, M.K., and McMahon, H.T. (2002). Snap-shots of clathrin-mediated endocytosis. Trends Biochem. Sci. *27*, 257–263.

Huttner, W.B., and Schmidt, A. (2000). Lipids, lipid modification and lipid-protein interaction in membrane budding and fission–insights from the roles of endophilin A1 and synaptophysin in synaptic vesicle endocytosis. Curr. Opin. Neurobiol. *10*, 543–551.

Huttner, W.B., and Schmidt, A.A. (2002). Membrane curvature: a case of endofeelin' em leader. Trends Cell Biol. *12*, 155–158.

Klingauf, J., Kavalali, E.T., and Tsien, R.W. (1998). Kinetics and regulation of fast endocytosis at hippocampal synapses. Nature *394*, 581–585.

Kuromi, H., and Kidokoro, Y. (2002). Selective replenishment of two vesicle pools depends on the source of Ca^{2+} at the Drosophila synapse. Neuron *35*, 333–343.

Llinas, R., Sugimori, M., and Silver, R.B. (1992). Microdomains of high calcium concentration in a presynaptic terminal. Science *256*, 677–679.

Maeno-Hikichi, Y., Chang, S., Matsumura, K., Lai, M., Lin, H., Nakagawa, N., Kuroda, S., and Zhang, J.F. (2003). A PKCε-ENH-channel complex specifically modulates N-type Ca^{2+} channels. Nat. Neurosci. *6*, 468–475.

Mayer, B.J. (2001). SH3 domains: complexity in moderation. J. Cell Sci. *114*, 1253–1263.

Murthy, V.N., and De Camilli, P. (2003). Cell biology of the presynaptic terminal. Annu. Rev. Neurosci. *26*, 701–728.

Neher, E., and Zucker, R.S. (1993). Multiple calcium-dependent processes related to secretion in bovine chromaffin cells. Neuron *10*, 21–30.

Neves, G., Gomis, A., and Lagnado, L. (2001). Calcium influx selects the fast mode of endocytosis in the synaptic terminal of retinal bipolar cells. Proc. Natl. Acad. Sci. USA *98*, 15282–15287.

Nguyen, J.T., Turck, C.W., Cohen, F.E., Zuckermann, R.N., and Lim, W.A. (1998). Exploiting the basis of proline recognition by SH3 and WW domains: design of N-substituted inhibitors. Science *282*, 2088–2092.

Pawson, T. (1995). Protein modules and signalling networks. Nature *373*, 573–580.

Ramaswami, M., Krishnan, K.S., and Kelly, R.B. (1994). Intermediates in synaptic vesicle recycling revealed by optical imaging of Drosophila neuromuscular junctions. Neuron *13*, 363–375.

Ringstad, N., Nemoto, Y., and De Camilli, P. (1997). The SH3p4/Sh3p8/SH3p13 protein family: binding partners for synaptojanin and dynamin via a Grb2-like Src homology 3 domain. Proc. Natl. Acad. Sci. USA *94*, 8569–8574.

Ringstad, N., Gad, H., Low, P., Di Paolo, G., Brodin, L., Shupliakov, O., and De Camilli, P. (1999). Endophilin/SH3p4 is required for the transition from early to late stages in clathrin-mediated synaptic vesicle endocytosis. Neuron *24*, 143–154.

Ringstad, N., Nemoto, Y., and De Camilli, P. (2001). Differential expression of endophilin 1 and 2 dimers at central nervous system synapses. J. Biol. Chem. *276*, 40424–40430.

Rizo, J., and Sudhof, T.C. (2002). SNARES and Munc18 in synaptic vesicle fusion. Nat. Rev. Neurosci. *3*, 641–653.

Roos, J., and Kelly, R.B. (1999). The endocytic machinery in nerve terminals surrounds sites of exocytosis. Curr. Biol. *9*, 1411–1414.

Sankaranarayanan, S., and Ryan, T.A. (2001). Calcium accelerates endocytosis of vSNAREs at hippocampal synapses. Nat. Neurosci. *4*, 129–136.

Schmidt, A., Wolde, M., Thiele, C., Fest, W., Kratzin, H., Podtelejnikov, A.V., Witke, W., Huttner, W.B., and Soling, H.D. (1999). Endophilin I mediates synaptic vesicle formation by transfer of arachidonate to lysophosphatidic acid. Nature *401*, 133–141.

Sheng, Z.H., Rettig, J., Cook, T., and Catterall, W.A. (1996). Calcium-dependent interaction of N-type calcium channels with the synaptic core complex. Nature *379*, 451–454.

Shupliakov, O., Low, P., Grabs, D., Gad, H., Chen, H., David, C., Takei, K., De Camilli, P., and Brodin, L. (1997). Synaptic vesicle endocytosis impaired by disruption of dynamin-SH3 domain interactions. Science *276*, 259–263.

Sicheri, F., Moarefi, I., and Kuriyan, J. (1997). Crystal structure of the Src family tyrosine kinase Hck. Nature *385*, 602–609.

Slepnev, V.I., and De Camilli, P. (2000). Accessory factors in clathrin-dependent synaptic vesicle endocytosis. Nat. Rev. Neurosci. *1*, 161–172.

Sparks, A.B., Hoffman, N.G., McConnell, S.J., Fowlkes, D.M., and Kay, B.K. (1996). Cloning of ligand targets: systematic isolation of SH3 domain-containing proteins. Nat. Biotechnol. *14*, 741–744.

Takei, K., and Haucke, V. (2001). Clathrin-mediated endocytosis: membrane factors pull the trigger. Trends Cell Biol. *11*, 385–391.

Teng, H., and Wilkinson, R.S. (2000). Clathrin-mediated endocytosis near active zones in snake motor boutons. J. Neurosci. *20*, 7986–7993.

Tong, A.H.Y., Drees, B., Nardelli, G., Bader, G.D., Brannetti, B., Castagnoli, L., Evangelista, M., Ferracuti, S., Nelson, B., Paoluzi, S., et al. (2002). A combined experimental and computational strategy to define protein interaction networks for peptide recognition modules. Science *295*, 321–324.

Verstreken, P., Kjaerulff, O., Lloyd, T.E., Atkinson, R., Zhou, Y., Meinertzhagen, I.A., and Bellen, H.J. (2002). Endophilin mutations block clathrin-mediated endocytosis but not neurotransmitter release. Cell *109*, 101–112.

Xu, W., Harrison, S.C., and Eck, M.J. (1997). Three-dimensional structure of the tyrosine kinase c-Src. Nature *385*, 595–602.

Yang, J., Ellinor, P.T., Sather, W.A., Zhang, J.F., and Tsien, R.W. (1993). Molecular determinants of Ca^{2+} selectivity and ion permeation in L-type Ca^{2+} channels. Nature *366*, 158–161.

Yoshihara, M., Adolfsen, B., and Littleton, J.T. (2003). Is synaptotagmin the calcium sensor? Curr. Opin. Neurobiol. *13*, 315–323.

Zhang, J.F., Randall, A.D., Ellinor, P.T., Horne, W.A., Sather, W.A., Tanabe, T., Schwarz, T.L., and Tsien, R.W. (1993). Distinctive pharmacology and kinetics of cloned neuronal Ca^{2+} channels and their possible counterparts in mammalian CNS neurons. Neuropharmacology *32*, 1075–1088.

Zhao, Z.-S., Manser, E., and Lim, L. (2000). Interaction between PAK and Nck: a Template for Nck Targets and Role of PAK Autophosphorylation. Mol. Cell. Biol. *20*, 3906–3917.